

# WAVE OVERTOPPING AT MALECÒN TRADICIONAL, LA HABANA, CUBA

Luis Fermin Cordova Lopez<sup>1</sup>, Daniela Salerno<sup>2</sup>, Fabio Dentale<sup>2</sup>, Alessandro Capobianco<sup>3</sup> and Mariano Buccino<sup>3</sup>

With the aim of redesigning the geometry of the *Malecòn*, a vertical face seawall protecting the northern waterfront of the city of La Habana, a wide experimental campaign was carried out. The latter was performed in the frame of a collaboration between the Government of the isle of Cuba and the CUGRI consortium, an Italian institution which joins the Universities of Salerno and Napoli “*Federico II*”. The different solutions investigated allowed both to detect the best solution for reducing the overtopping and to assess the role of wave setup and low frequency components of the incoming wave spectrum on the predictions of the mean overtopping rate. The stability of two nearshore structures designed to protect the seawall has also been assessed.

*Keywords:* wave overtopping; physical model tests; vertical seawall

## INTRODUCTION

One of the peculiarities of La Habana, capital of the Republic of Cuba, is the vertical seawall, known as the *Malecòn* (Fig. 1), protecting the northern part of the city centre from the wave action.

Recently, the climatic changes have caused an increase of the magnitude of the most severe meteorological events, including cyclones and hurricanes reaching the isle of Cuba during the winter. This has induced the *Malecòn* to be often overtopped by waves endangering human lives and historical buildings.

For this reason the Cuban Government has looked for a solution reducing the risk of flooding and respecting the enormous value of the site. In particular, at the beginning of 2013, scientists and engineers of the *Centro de Investigaciones Hidráulicas (CiH)* of the *Instituto Superior Politécnico “Jose Antonio Echevarria”* have presented a desk study where a number of solutions were considered, including a weak increase of the wall freeboard, curvature of the outer profile and placement of protective structures, such as berms and detached low-crested breakwaters.

With the aim of investigating the effects of each mitigating solution a series of physical model tests were planned to be performed. The latter were commissioned to the *Consorzio interUniversitario per la previsione e prevenzione dei Grandi Rischi (CUGRI)*, which joins the Universities of Napoli “*Federico II*” and Salerno (Italy).

This paper describes the experimental campaign and discusses the most interesting results of the tests. Given the shallow foreshore affecting the *Malecòn*, particular attention has been drawn to the role of wave set up and long wave components of the incident wave spectrum on the predictability of the mean overtopping discharge.

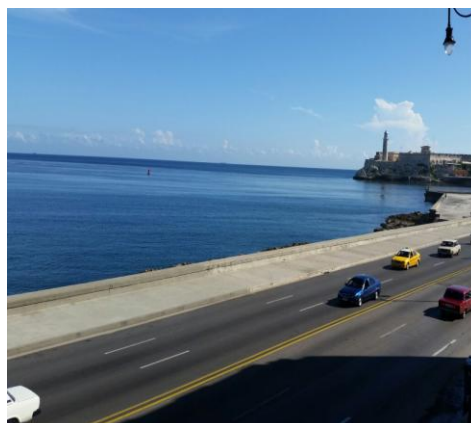


Figure 1. View of the Malecòn.

## WAVE OVERTOPPING AT VERTICAL STRUCTURES

Wave overtopping is a deeply investigated topic in the field of coastal engineering and several predictive expressions have been suggested by researchers.

---

<sup>1</sup> Centro de Investigaciones Hidráulicas of the Instituto Superior Politécnico “Jose Antonio Echevarria” La Havana, Cuba

<sup>2</sup> Department of Civil Engineering, University of Salerno, Via Giovanni Paolo II, 132 - 84084, Fisciano, Italy

<sup>3</sup> Department of Civil, Architectural and Environmental Engineering, University of Naples “Federico II”, Via Claudio, 21 - 80125, Napoli, Italy

Franco and Franco (1999) proposed a simple exponential form based on a wide series of random wave experiments on caisson breakwaters:

$$\frac{q}{\sqrt{gH_{m0}^3}} = \alpha \cdot \exp\left(-\beta \cdot \frac{R_c}{H_{m0}}\right) \quad (1)$$

in which  $q$  is the mean overtopping discharge,  $g$  is the gravity acceleration,  $R_c$  is the crest freeboard and  $H_{m0}$  is the incident spectral significant wave height at the toe of the breakwater. The parameters  $\alpha$  and  $\beta$  are function of a number of hydraulic and structural variables, including wave obliquity, short crestedness and curvature of the outer profile of the caisson crown wall. A contribution to the prediction of wave overtopping has been provided by the EC research project CLASH (De Rouck et al., 2009), as well as from several national programs. The EurOtop Manual (2007) takes account the new results and provides a useful guide for practical applications.

For the case of simple un-protected vertical seawalls, two formulae have been proposed corresponding to two hydrodynamic conditions and namely “*pulsating*” and “*impulsive*”: the former occurs when waves are both little steep and relatively small in relation to the local depth, the latter when waves are larger enough in relation to local water depths to break often violently against the wall. In order to proceed with assessment of wave overtopping, it is necessary first to determine the dominant overtopping regime (impulsive or non-impulsive) for a given structure and sea state. An “*impulsiveness*” parameter has to be defined:

$$h_* = 1.35 \cdot \frac{h_s}{H_{m0}} \cdot \frac{2\pi \cdot h_s}{gT_{-10}^2} \quad (2)$$

where  $h_s$  is the mean water depth at the toe of the wall and  $T_{-10}$  is the mean spectral period based on the moments of order -1 and 0 of the incident power spectrum. Non impulsive conditions dominate when  $h_* > 0.3$ , and impulsive conditions are observed when  $h_* < 0.2$ .

For  $0.2 \leq h_* \leq 0.3$ , overtopping should be predicted for both non impulsive and impulsive conditions, and the larger value assumed.

For impulsive conditions, which are those of interest for the present study, the predictive equations are:

$$\frac{q}{h_*^2 \sqrt{gh_s^3}} = 1.5 \cdot 10^{-4} \cdot \left(\frac{h_* R_c}{H_{m0}}\right)^{-3.1} \quad (3)$$

if  $0.03 < h_* R_c / H_{m0} < 1$ , and:

$$\frac{q}{h_*^2 \sqrt{gh_s^3}} = 2.7 \cdot 10^{-4} \cdot \left(\frac{h_* R_c}{H_{m0}}\right)^{-2.7} \quad (4)$$

If  $h_* R_c / H_{m0} < 0.02$ .

For  $h_* R_c / H_{m0}$  ranging between 0.02 and 0.03, the maximum between the two previous formulae should be used.

EurOtop also provides a decision tree to assess the effect of the curvature of the outer face of the wall; the reduction ratio:

$$K = \frac{[q]_{curve}}{[q]_{vert.}} \quad (5)$$

can be calculated as a function of the non dimensional crest freeboard  $R_c / H_{m0}$  as well as on the main geometric features of the concave structure.

A further design tool was suggested by Goda (2009) who proposed a set of formulae valid for both vertical and inclined structures, based on the functional form:

$$\frac{q}{\sqrt{gH_{m0}^3}} = \exp\left(A + B \cdot \frac{R_c}{H_{m0}}\right) \quad (6)$$

where for any inclination of the front face of the structure, the parameters A and B are functions of the foreshore slope and of the wave height to depth ratio.

**LABORATORY STUDY**

**Facility**

A series of 1:30 physical model tests have been carried out at the Random wave TAnk (RATA) of the Department of Civil, Architectural and Environmental Engineering (DICEA) of the University of Naples “Federico II”. The facility is 36m long, 18m wide, 1.2m deep and is provided with 16 independent piston type wavemakers, capable of simulating both regular and irregular wave trains with different angles of propagation and (for random waves) directional spreading.

The basin has been partitioned to form a 18.37m x 1.54m channel with concrete walls, where the experiments have been carried out (Fig. 2). Further walls have been constructed along the generation line to separate the tank into a dry zone, needed for the observation of the tests, and a wet zone, which has been filled with water. The purpose of this area was to create a large additional volume of fluid to compensate for the losses associated with the overtopping process and avoid any variation of water level in the channel.

**Foreshore**

A 230m long portion of foreshore (7.67m in the model) has been reproduced in the flume (in concrete); it brought the sea floor from a depth of 18.72m below the MWL to the toe of the Malecòn seawall, which is nearly at 1.70m (Fig. 3).

After a 6.00m long flat area (model scale), the bathymetry encompasses a mild stretch with a 4.1% slope, followed by a step inclined by 1:3 and an upper zone made up on 2 parts with a slope of 8.6% and 6% respectively.

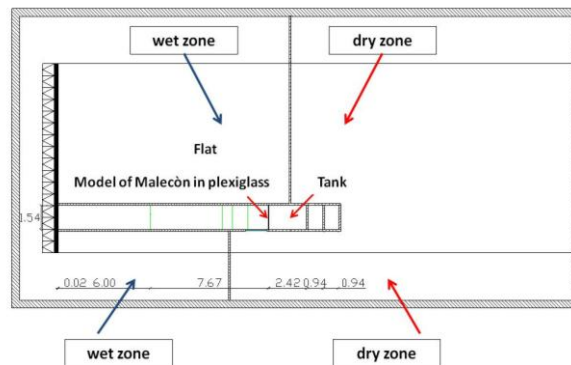


Figure 2. Partitioning of the RATA wave basin.

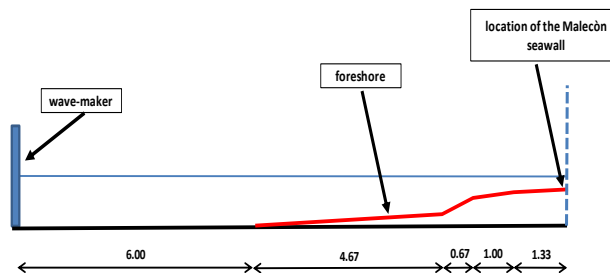


Figure 3. View of the foreshore.

**Foreshore**

In addition to its current configuration, (vertical wall with  $R_c$  of + 3.96m relative to the MWL (Fig. 4.a)), the Malecòn seawall has been tested with different clearances, and namely + 4.46m and +

4.96m relative to the MWL. These values of  $R_c$  have also been used with a curve layout. Accordingly, 6 models of seawall (3 curve and 3 vertical) have been employed.

### OVERTOPPING TESTS

Along with the variation of crest freeboard and outer profile, also the effect of rubble mound berms and detached low crested breakwaters (*LCB*) on the amount of overtopping has been investigated. At the end of this paper, which focuses mainly on the results of the experiments conducted on “un-protected walls”, preliminary outcomes relative to the efficiency of berms are discussed.

Three berm geometries have been tested, all with a front slope angle of 1:1.5 (Fig. 5). The first (*Berm 1*) had the freeboard ( $F$ ) at +3.28m above the MWL, whereas the width ( $B$ ) equaled 5m; the second (*Berm 2*) was at  $F = +2.28\text{m}$  with a  $B = 20\text{m}$ . The third (*Berm 3*) had  $F = +1.73\text{m}$  and  $B = 30\text{m}$ . Each berm has been tested with a vertical wall with  $R_c = 3.96\text{m}$  and with a curved wall with  $R_c = 4.46\text{m}$ .

The geometric characteristics of the berms have been derived from the desk study presented by the Centro de Investigaciones Hidráulicas of the Instituto Superior Politécnico “Jose Antonio Echevarria”, concerning the possible protective structures for the Malecón.

Two rises of the mean sea level have been considered; one corresponds to the scenario of the Wilma hurricane (occurred in 2005), the other is associated with a 50 years return period storm (Table 1).

For each value of the still water depth, 8 JONSWAP driven random sea states have been run, with a duration of 1000 waves. 4 values of the spectral significant wave height ( $H_{m0}$ ) at the paddle have been used, namely 2.7m, 4.0m, 5.4m and 6.5m, with two peak periods ( $T_p = 10\text{s}$  and  $12\text{s}$ ).

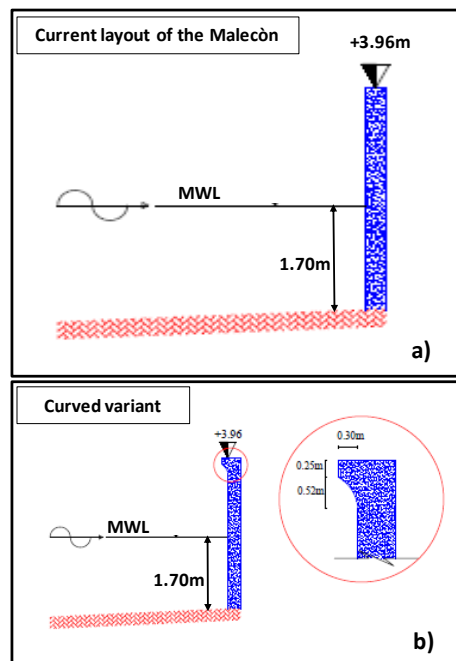


Figure 4.a). Current layout of the Malecón seawall. b) curved variant.

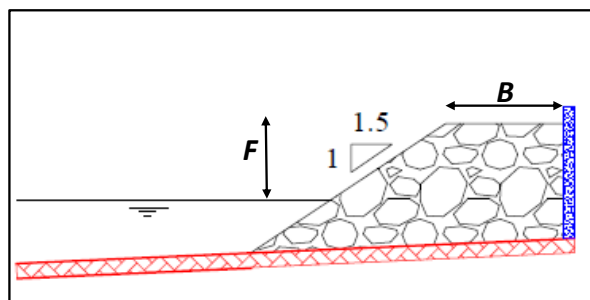


Figure 5. Berm protected vertical seawall.

Scenario	Storm surge [m]	Tide [m]	Climatic change [m]	Total [m]
50 years RP	1.06	0.40	0.27	1.73
Wilma Hurricane	1.53	0.48	0.27	2.28

Prior performing the overtopping tests, a 1:20 spending beach made of plywood has been mounted rear the foreshore (Fig. 3); the incident wave conditions at the toe of the wall have been then measured without the wall, via a twin-wire resistive wave probe sampled at 25Hz (Fig. 6).



**Figure 6. Tests for wave measurements at the toe of the wall.**

Further 4 probes were placed on the flat bottom in front of the bathymetry to separate incident and reflected waves according to the Zelt and Skjelbreia (1992) method.

To measure the mean overtopping discharge,  $q$ , the spending beach has been removed and a  $1\text{m}^3$  reservoir has been built leeward the seawall. The water overpassing the structure was collected in the reservoir and then conveyed back to the wet zone (Fig. 2) by means of 2 submersible pumps of the overall capacity of 800 l/min. The pumped water passed through an electromagnetic flowmeter, where the volume of fluid was progressively computed (Fig. 7).



**Figure 7. View of the electromagnetic flow meter.**

The water volume in the reservoir at the beginning ( $V_b$ ) and at the end ( $V_e$ ) of each test was controlled by a supplementary wave probe located in the collecting tank and sampled at 25 Hz. Thus, the overtopping rate has been finally obtained as:

$$q = \frac{V_{pumped} + V_e - V_b}{D_t} \quad (7)$$

where  $D_t$  is the duration of the test.

### STABILITY TESTS

After the wide experimental campaign aimed to assess the overtopping performance of the wall, it was concluded that a reasonable solution to reduce overpassing with a low impact on the landscape was to increase the height of the structure by 0.5m, curveting at the same time the upper part of the outer face. This layout has been used in the stability tests.

As this expedient is not sufficient to guarantee an appropriate reduction of the rate of overtopping, additional nearshore structures which reduce the intensity of wave attacks, have been included.

Although the Berm 3 induces the largest reduction in the overtopping rate, for economic reasons the Berm 1 has been preferred. The latter has been employed for the stability tests together with a detached low crested breakwater. The two solutions have been analyzed separately.

The detached low crested breakwater (LCB) (Fig.8) is placed on a mean water depth of 5.05m and has the crown 3.28m above the MWL. The crest width is 12.0m and both the front and the rear slopes have an inclination of 2:3. For the armor layer, randomly placed concrete cubes on two rows have been designed, with a weight of 30 tons.

The emerged berm (EB) (Fig.5) is located on a depth of 2.30m below the MWL. For the armor, randomly placed concrete cubes with a weight of 2.3 tons have been designed.

Table 2 summarizes the design characteristics of the structures. In Table 3 the nominal diameter  $D_{n,50}$  is defined as:

$$D_{n,50} = \frac{W_{50}}{\gamma_c} \quad (8)$$

where  $W_{50}$  is the median weight of the armor units and  $\gamma_c$  is the weight per unit volume of concrete, assumed equal to 2.4 tons/m<sup>3</sup>.

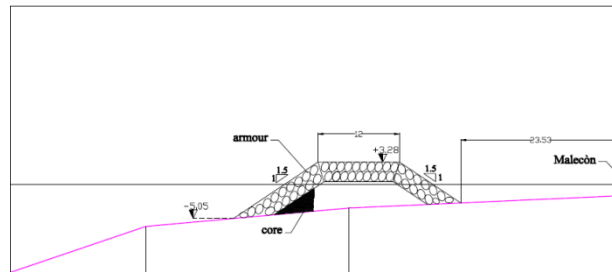


Figure 8. Scheme of the detached Low Crested Breakwater.

Table 4 shows the design values of the significant wave heights at the mean water depth of 20m, along with the respective Return Period (RP). For these tests the waves corresponding to R = 20 and 100 years have been employed.

Both the wave heights have been associated with a peak period  $T_p = 10s$ , corresponding to the smallest value considered in the original desk study on the response of the Malecón Tradicional. This to maximize wave steepness.

Three different water levels have been considered and namely:

- MWL;
- MWL +1.73m, which corresponds to the climate conditions (storm surge + tide) referred to as “50 years return period”;
- MWL +2.28m, which corresponds to the climate conditions (storm surge + tide) referred to as “Hurricane Wilma”.

Altogether, 6 storm conditions have been employed, according to Table 5.

Table 2. Characteristics of nearshore structures					
Structure type	Freeboard from MWL [m]	Crown width [m]	Front slope	Rear slope	Depth at the toe from the SWL [m]
Berm	+3.28	5.00	2V:3H	---	2.30
Detached Low crested breakw	+3.28	12.00	2V:3H	2V:3H	5.05

Structure type	W50 [tons]	Dn,50 [m]
Berm	2.30	0.99
Detached Low crested breakw	30	2.30

Return Period [years]	H <sub>m0</sub> [m]
5	4.0
20	5.4
100	6.5

Storm code	H <sub>m0</sub> [m]	T <sub>p</sub> [s]	Water Depth [m]
A	5.4	10	18.72 (MWL)
B	6.5	10	18.72 (MWL)
C	5.4	10	MWL+1.73
D	6.5	10	MWL+1.73
E	5.4	10	MWL+2.28
F	6.5	10	MWL+2.28

For the armors of the nearshore structures, small concrete cubes on two rows have been used. To account for the difference in the specific weight between salt and fresh water, a little correction to the scaling has been applied.

The principle used is that of having the same stability number in the model and in the prototype:

$$\left[ \frac{H_{m0}}{\Delta D_{n,50}} \right]_{prot.} = \left[ \frac{H_{m0}}{\Delta D_{n,50}} \right]_{mod.} \quad (9)$$

in which the specific gravity  $\Delta$  equals:

$$\Delta = \frac{\gamma_c}{\gamma_w} - 1 \quad (10)$$

where the weight per unit volume of water equals 1.03 tons/m<sup>3</sup> in prototype and 1.00 tons/m<sup>3</sup> in the model (fresh water). Thus from the Equation (9), the proper scaling rule for D<sub>50</sub> is:

$$(D_{50})_{mod.} = \frac{(H_{m0})_{mod.}}{(H_{m0})_{prot.}} \cdot \frac{(\Delta)_{prot.}}{(\Delta)_{mod.}} \cdot (D_{50})_{prot.} \cong 0.95 \frac{(D_{50})_{prot.}}{30} \quad (11)$$

and hence:

$$(W_{50})_{mod.} \cong 0.86 \frac{(W_{50})_{prot.}}{30^3} \quad (12)$$

Based on the Equation (12), we obtain for LCB:

$$(W_{50})_{mod.} = 0.955kg \quad (13)$$

whereas for EB:

$$(W_{50})_{mod.} = 0.073kg \quad (14)$$

The experimental values of the median weights are 1.010 kg for LCB and 0.0746 kg for EB, which are slightly larger than what expected. This implies (Eq.12) that the actual prototype values of the weights tested are 31.7 tons for LCB and 2.34 tons for EB.

Each protection structure (LCB and EB) has been loaded with the six design storms of Table 5. Each wave attack lasted 3,000 peak periods, i.e. 5490s.

As shown in Figures 9 and 10, different colours have been used to paint the three parts of the structures (front slope, crest and for LCB rear slope). High resolution photos were taken before and after each storm to assess the level of damage N<sub>od</sub>.

The latter is defined as the number of units displaced out of a strip wide D<sub>50</sub> along the longitudinal axis of the structure. After counting the number of units displaced in the entire flume width (N<sub>d</sub>), the following formula has been employed:

$$N_{od} = \frac{N_d D_{50}}{b} \quad (15)$$

where b is the width of the flume.

According to the client's design, the following requirements needed to be met for the structure response to be considered acceptable:

- N<sub>od</sub> does not overcome 0.5 with respect to the 20 years RP wave attacks (Tests A,C,E)
- N<sub>od</sub> does not overcome 1.5 with respect to the 100 years RP wave attack (Tests B,D,F).



Figure 9. Pre-storm photo of LCB.



Figure 10. Pre-storm photo of EB.

## RESULTS

Due to the shallow foreshore, incoming waves experienced significant breaking before reaching the structure. Accordingly, the power spectrum resulted pretty broad-banded (Figure 11). In order to investigate the effects on the mean overtopping discharge of the wave energy distribution in the

frequency domain, the spectral function has been conventionally divided into the following components:

- Wave setup (or set-down), corresponding to the DC component of the wave spectrum or the average of the wave oscillations in the time domain (Longuet-Higgins and Stewart, 1965; Calabrese et al., 2003; Calabrese et al., 2008).
- Long waves domain, including the spectral components with frequency larger than 0 (wave set-up) and lower than half the offshore peak frequency,  $f_p$ ;
- Short waves domain corresponding to frequencies included between  $0.5 f_p$  and the Nyquist frequency  $f_N$ .

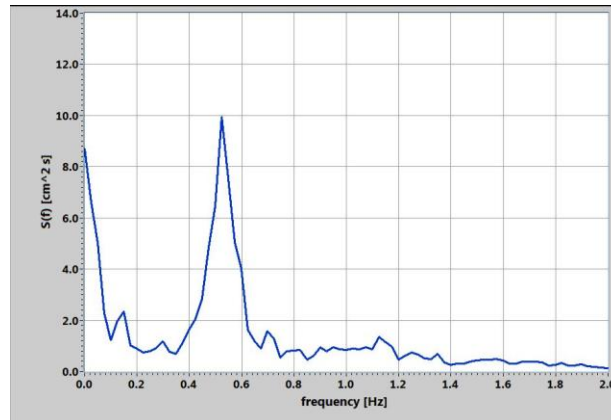


Figure 11. Example of wave power spectrum acquired at the location of the wall.

This section aims to provide a deeper insight on the influence of wave parameters (height, period and setup) on the quality of prediction of the mean overtopping discharge. The Figures 12 and 13 display the experimental data on the characteristic planes of the Franco and Franco (1994) and EurOTOP equations. Here only the short waves have been considered; accordingly the crest freeboard  $R_c$  is computed from the still water level, leaving the wave setup out of consideration.

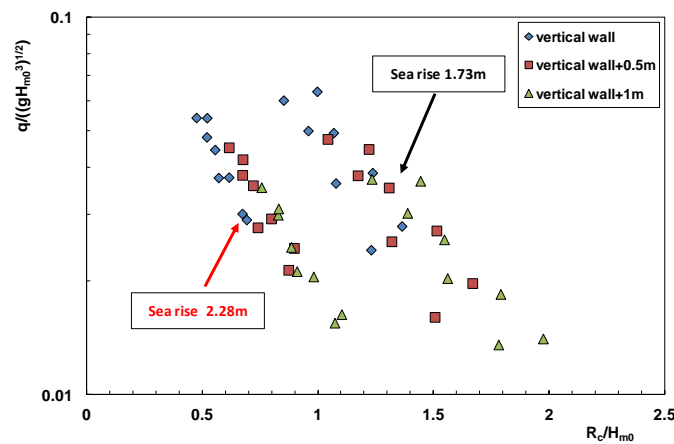


Figure 12. Experimental data on the Franco and Franco (1994) characteristic plane. Short wave parameters have been used.

In Figure 12, the experimental points split into two clouds, depending on the (still) water depth at the wall; conversely in Figure 13 they have a unique trend, which though overwhelms the EurOTOP predictions (black solid curve). Data can be conveniently fitted via the power form:

$$\frac{q}{h_w^2 \sqrt{gh_s^3}} = a \cdot \left( \frac{h_w R_c}{H_{m0}} \right)^b \tag{16}$$

with  $a = 0.041$  and  $b = -1.63$  (dashed red curve). The formula has a corrected  $R^2$  statistics equal to 0.82.

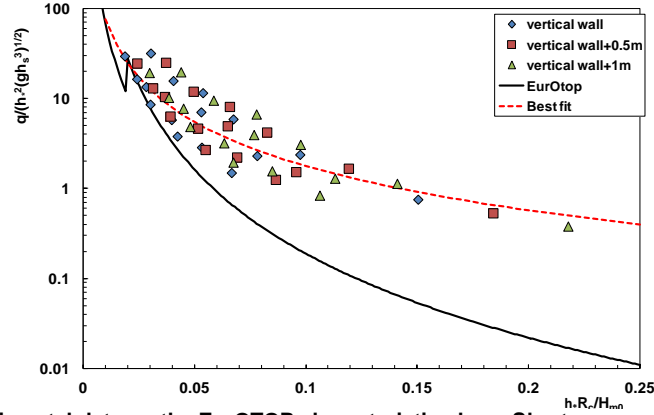


Figure 13. Experimental data on the EurOTOP characteristic plane. Short wave parameters have been used. Wave setup has not been considered.

wave parameters have been used. Wave setup has not been considered

It is worth noticing that the application of Equation (16) requires in fact the knowledge of the spectral distribution function in the short wave domain, which is necessary for the mean period  $T_{-10}$  to be calculated. In case only the amount of short wave energy ( $H_{m0}$ ) were available, along with its peak frequency, the quality of the estimates would be some poorer; after calculating the quantity  $h^*$  via the *offshore peak period* and refitting the data, an  $R^2 = 0.77$  was achieved. As expected the variation is not dramatically significant, as  $T_{-10}$  is scarcely influenced by the high frequency components of the power spectrum.

The inclusion of the wave setup at the location of the seawall (measured in absence of structure) proved rather beneficial; in Figure 14 data appears less scattered than in Figure 13, although the EurOTOP formula still lies below the experimental values; the best fit power form is now:

$$\frac{q}{h_s^2 \sqrt{g h_s^3}} = 0.036 \cdot \left( \frac{h_s R_c}{H_{m0}} \right)^{-1.63} \quad (17)$$

in which the value of wave set-up has been included either in  $R_c$  or in  $h^*$  or in  $h_s$  and the  $T_{-10}$  of the short wave spectrum has been used. The  $R^2$  statistics is 0.90, indicating a good prediction power.

It is nice to observe that when the offshore wave period is substituted to  $T_{-10}$ , the determination coefficient slightly increases, reaching 0.91.

When the entire power spectrum is employed, including long waves, the data scatter further reduces and the EurOTOP curve now provides reasonable estimates (Figure 15). The power form of Equation (16) can be still effectively fitted to the data with  $a = 0.00886$  and  $b = -2.0518$ . The  $R^2$  statistics is 0.973, meaning that almost all the variance of data is explained.

When the offshore peak period is used instead of  $T_{-10}$ , the performance of Equation (17) remains slightly worsen, with  $R^2$  dropping to 0.93. Table 6 provides a summary of the performed regression analyses. Last column gives the standard deviation of the difference between measured and predicted flow rates (at prototype scale).

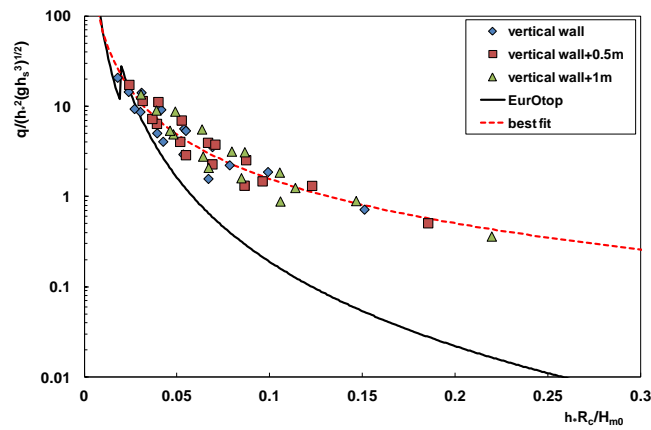


Figure 14. Experimental data on the EurOTOP characteristic plane. Short wave parameters have been used. Wave setup included.

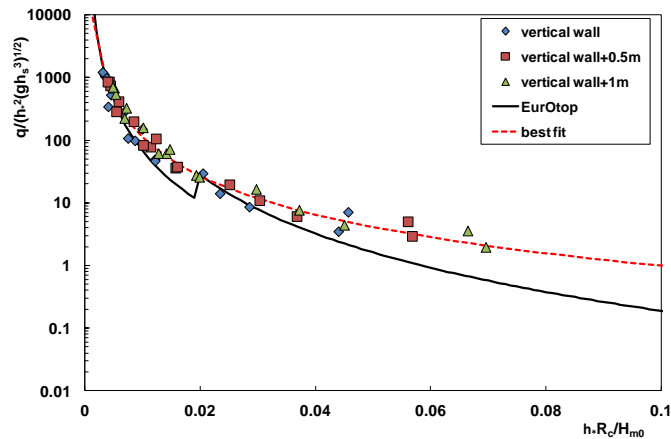


Figure 15. Experimental data on the EurOTOP characteristic plane. The entire spectrum. Wave setup included.

Table 6. Performance of the Eq.(16)				
Wave parameters	a	B	R <sup>2</sup>	Residual st. dev. [m <sup>3</sup> /s/m]
Short- no set up	0.041	-1.630	0.821	0.107
with Tp	0.053	-1.629	0.767	0.122
Short + set up	0.036	-1.636	0.899	0.079
with Tp	0.055	-1.550	0.906	0.0760
Entire + setup	0.009	-2.015	0.973	0.0416
with Tp	0.040	-1.619	0.932	0.0661

Similarly to what observed for the mean overtopping discharge, also the prediction of the effect of the seawall curvature was found to be significantly dependent on the wave parameters employed and, accordingly, on the information available at the design stage. If neither long wave energy nor wave setup are known, the EurOTOP procedure gives reduction coefficients K rather lower than the measured ones (Figure 16).

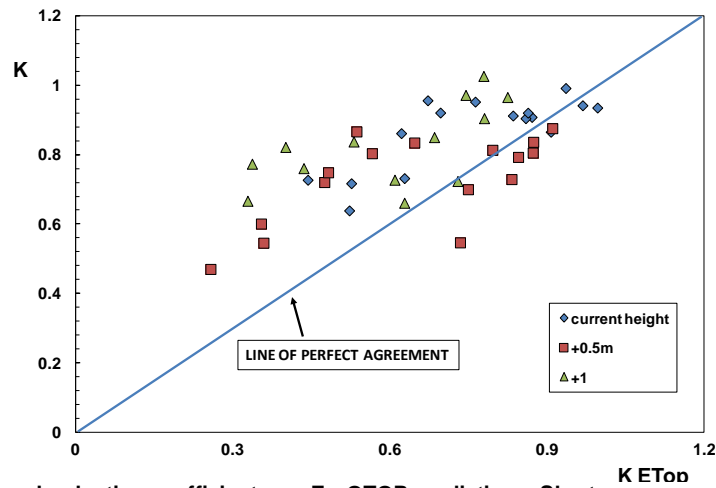


Figure 16. Measured reduction coefficients vs. EurOTOP predictions. Short wave parameters have been used, excluding wave setup.

On the other hand, if the full energy band is used, and the wave setup is included in the calculation of the crest freeboard, both the amount of overestimates and the scatter of data around the prediction line are observed to reduce (Figure 17).

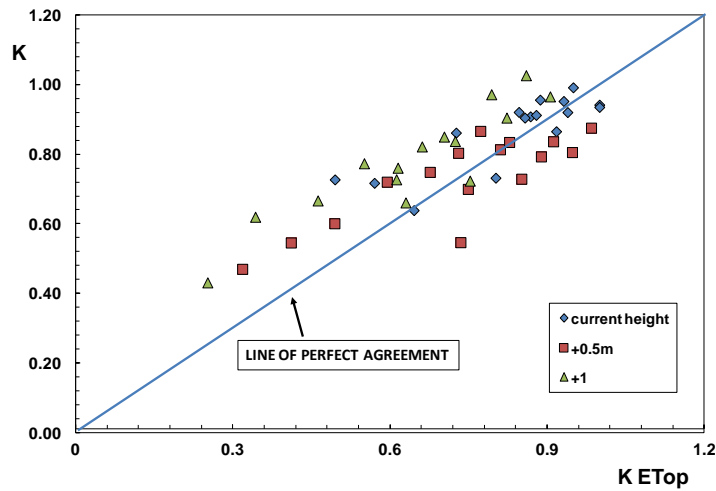


Figure 17. Measured reduction coefficients vs. EurOTOP predictions. Full spectrum wave parameters have been used, including wave setup.

Table 7 reports, for the different wave parameters, the mean and the standard deviation of the difference between measured and predicted values of K. The long waves energy appears now to play a leading role compared to wave setup.

Table 7. Quality of EurOTOP prediction of the seawall curvature effect		
Wave parameters	mean	St.dev.
Short- no set up	0.135	0.149
Short + set up	0.115	0.148
Full + setup	0.055	0.108

The analyses on the berm effect indicates that the degree of protection offered by the rubble mound structure strongly decreases with growing the wave height. An example is given in Figure 18, which refers to the vertical seawall at the current height, with the offshore peak period  $T_p = 12s$  under the Wilma scenario. The graph displays the rate of reduction of the mean discharge (calculated as the ratio between the difference of the mean discharge without and with the berm, and the mean discharge in absence of berm) vs. the offshore wave height.

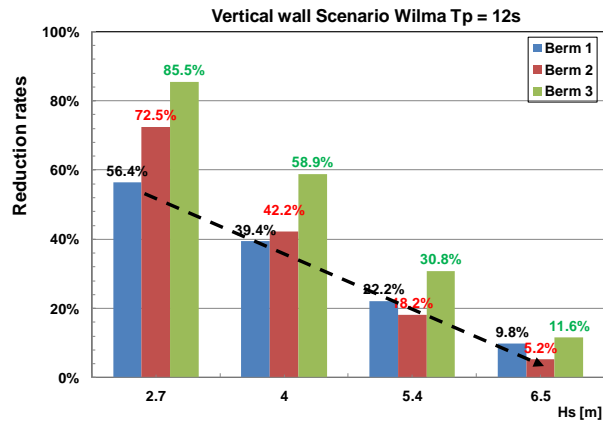


Figure 18. Relative rate of reduction of the mean discharge as function of the berm geometry and the offshore wave height.

For the Berm 3, for example, the degree of protection drops from 85.5% for the offshore wave height 2.7m to 11.6% for 6.5m.

As far as the stability tests are concerned, both the structures failed under the design storms; in wide zones of the front slope and crest, the armor was completely removed. LCB heavily failed under the attacks A and B of Table 5; during the wave attacks the front slope collapsed and moved significantly seaward. On the other hand, EB experienced failure with higher water levels.

Figures 19 and 20 show photos pre and post storm.

The main variable leading to the structures failure seems to be the position of the breaker line. For LCB the latter is very close to the front slope under the conditions A and B, whereas for EB this occurs for the higher water levels.



Figure 19. Pre-storm (upper) and post-storm (lower) photos for LCB. Storm condition B.



Figure 20. Pre-storm (upper) and Post-storm (lower) photos for EB. Storm condition B.

## CONCLUSIONS

In the frame of a leading project for the protection of the waterfront of the city of La Habana (Cuba), a wide experimental study has been carried out at the DICEA Dept. of the University of Naples “Federico II”. Physical model tests have been carried out to assess the average amount of water overtopping the historical vertical face seawall called Malecón Tradicional, as well as implement possible design improvements, such as curvature of the outer profile, variation of freeboard, placement of protective rubble mound structures (berms and low crested detached breakwaters).

This paper discusses preliminary outcomes of the experiments, with a main focus on the effect of the shallow water wave parameters (wave height, period and wave setup) on the prediction of the mean overtopping rate at unprotected layouts.

It has been found that a proper knowledge of the whole wave energy and setup at the wall (including low frequencies) leads the overtopping process to be highly predictable (see Table 6); moreover, under this condition, the measured value of the overtopping rates agree reasonably with the predictions of the EurOTOP formula (Figure 15). However, when only high frequency spectral parameters are available and/or a reliable estimate of the wave setup at the location of the wall is not disposable, the scatter of data increases dramatically and the EurOTOP formula may give significant underpredictions of the real flow rates.

In these cases, Table 6 may supply engineers an order of magnitude predictor, along with an estimate of the residual scatter.

Figures 16 and 17 suggest that the knowledge of the long wave energy at the wall also influence the prediction of the effect of a curved wall. Similarly to Table 6, Table 7 shows that a complete knowledge of the wave climate practically halves the scatter of data.

These findings are globally in agreement with those van Gent and Gianrusso (2003), who used though only data from numerical models.

First results on the degree of protection offered by berms indicate it is extremely reduced for the most energetic incoming storms (Figure 18).

The stability tests conducted on the protective structures suggested that:

- The LCB should be moved shorewards and armored with concrete units which provide a good degree of interlocking (Figure 21);
- The EB should be armored either with heavier cubes or with interlocking units;
- Much attention should be paid in the design of the protection toes.



Figure 21. View of the LCB with concrete units with a large degree of interlocking.

#### REFERENCES

- Calabrese, M., Vicinanza, D. and Buccino, M. (2003). "2D wave setup behind low crested and submerged breakwaters". *Proceedings of the International Offshore and Polar Engineering, ISOPE 2003*, pp. 2176-2181.
- Calabrese, M., Buccino, M. and Pasanisi, F. (2008) "Wave breaking macrofeatures on a submerged rubble mound breakwater". *Journal of Hydro-Environment Research*, 1 (3-4), 216-225.
- De Rouck, J., Verhaeghe, H., and Geeraerts, J.(2009). "Crest Level Assessment of coastal Structures: general overview". *Coastal Engineering, ELSEVIER*, 56(2), 99-107.
- EurOtop, (2007). "Wave overtopping of sea defences and related structures: Assessment manual", T. Pullen, N. W. H. Allsop, T. Bruce, A. Kortenhaus, H. Schüttrumpf, and J. W. van der Meer, eds., Environment Agency, UK/ENW Expertise Netwerk Waterkeren, NL/KFKI Kuratorium für Forschung im Küsteningenieurwesen, Germany, <http://www.overtopping-manual.com> (Mar. 11, 2011).
- Franco, C. and Franco, L. (1999) "Overtopping formulas for caisson breakwaters with non-breaking 3D waves". *J. Waterw. Port Coast. Ocean Eng. ASCE*, 125, 98–107.
- Goda, Y. (2009). "Derivation of unified wave overtopping formulas for seawalls with smooth, impermeable surfaces based on selected CLASH datasets." *Coastal Engineering., ELSEVIER*, 56(4), pp. 385–399.
- Longuet-Higgins, M.S., Stewart, R.W. (1964). "Radiation stresses in water waves; a physical discussion, with applications" *Deep-Sea Research and Oceanographic Abstracts*, 11 (4), 529-562.
- Van Gent, M. R.A and Gianrusso C.C. (2003) "Influence of low frequency waves on wave overtopping". CLASH Report and Delft Hydraulics Rep. H4297.Delft Hydraulics, the Netherlands.